KSCE Journal of Civil Engineering (2019) 23(3):992-999
Copyright ⓒ2019 Korean Society of Civil Engineers
DOI 10.1007/s12205-019-1034-x

Environmental Engineering
pISSN 1226-7988, eISSN 1976-3808
www.springer.com/12205

Nano-pyrite as a Reductant to Remove Chromium in Groundwater

Nurul Aqilah Abdul*, Suhaimi Abdul-Talib, and Amnorzahira Amir*****

Received May 23, 2018/Revised August 7, 2018/Accepted August 29, 2018/Published Online January 2, 2019

Abstract

Removal of total chromium (Cr_T) by nano-pyrite (nano-FeS_2) was investigated under different environmental conditions. Size of nano-FeS_2 was in the range of 50–100 nm and it contained Fe and S. Removal kinetic rate constant of Cr_T was significantly dependent on the suspension pH and concentrations of Cr_T, nano-FeS_2 and Humic Acid (HA). The removal kinetic rate constant of Cr_T by nano-FeS_2 was decreased as the concentration of Cr_T was increased (0.43–0.29 min^{-1}), while contradict kinetic result was observed as the concentration of nano-FeS_2 was increased (1.11–2.78 min^{-1}). The removal kinetic rate constant of Cr_T was significantly increased as the suspension pH increased (0.86–3.0 min^{-1}). However, the removal kinetic rate constant of Cr_T was significant decreased in the present of HA (1.25–0.25 min^{-1}). The removal kinetic rate constant of Cr_T by nano-FeS_2 was strongly controlled by the reactive surface area of nano-FeS_2. Identification of the formation of $FeCr_2O_4$ on the surface of nano-FeS_2 reveals that adsorption, complexation and reduction reactions may occur during the removal reaction. This study provides fundamental knowledge on the fate of Cr under different groundwater conditions. Findings from this study can be used to enhance remediation technology of removal heavy metals from groundwater.

Keywords: *chromium, humic acid, groundwater, nano-FeS_2, removal kinetic rate constant*

1. Introduction

Abundant existence of Hexavalent chromium (Cr^{6+}) was reported in groundwater and it is listed as a priority pollutant in the list of toxic and hazardous pollutant in United State Environmental Protection Agency (USEPA) (Ertani *et al*., 2017; Lasheen *et al*., 2013). Cr^{6+} is widely used in industries such as the production of stainless steel, leather tanning, electroplating and chemical industries and it is released into environment without proper treatment (Aftabtalab and Sadabadi, 2015; Lasheen *et al*., 2013; Liu *et al*., 2015). Literature have reported that the Cr^{6+} concentration was detected beyond the allowable limit concentration (0.1 mg/L) in rivers and groundwater and this situation has become a serious concern to environmentalists (Panagiotakis *et al*., 2015). Cr^{6+}can be persistently present in groundwater with high mobility. Due to this reason, source of drinking water may be contaminated and become harmful to human health. Exposure of Cr^{6+} to human health may lead to liver damage, pulmonary congestion, edema and skin irritation (Mohan and Pittman, 2006; Vinuth *et al.*, 2015). Therefore, USEPA recommended that the allowable limit for Cr^{6+} in the drinking water guideline is set to less than 100 µg/L (Mohan and Pittman, 2006).

Current remediation technology of Cr^{6+} in groundwater focus on chemical treatment (e.g., ion exchange and adsorption) (Taylor, 2015) and biological treatment (e.g., bioreduction and bioaccumulation) (Risk and Agency, 2000). The main purpose of these treatments is to reduce toxic Cr^{6+} to chromium (III) (Cr^{3+}). Cr^{3+} is relatively non-toxic and it has low mobility in groundwater compared to Cr^{6+} (Kantar *et al*., 2015). Chemical treatment using iron reductant (Fe^{2+}) is one of the predominant methods to reduce Cr^{6+} to Cr^{3+} in groundwater. Literatures have reported that pyrite (FeS_2) is one of the reactive iron reductant in soil and groundwater and it can effectively remove organic and inorganic pollutants in groundwater (Wernberg, 2017). Recently, literatures have reported that nano-FeS_2 can be been found in magmatic rocks, hydrothermal deposits (Bae *et al*., 2012; Demoisson *et al.*, 2007; Demoisson *et al*., 2005) and in an aquifer located at the base of the flow system and 7m below the water table (Sharma, 2001; Wernberg, 2017). It has been reported that Cr^{6+} removal by nano-FeS_2 was influenced by the reactive site of ferrous iron (Fe^{2+}) and disulfide (S_2^{2-}) (Kantar *et al*., 2015a). However, the removal of Cr by nano-FeS_2 was significantly affected by the physicochemical properties of groundwater.

Literatures have reported that pH, Natural Organic Matter (NOM) and Oxidation-Reduction Potential (ORP) were significantly influenced the fate of Cr in groundwater (Banks *et al*., 2006; Porsch

---

*Research Assistant, Bioremediation Research Centre (myBioREC), The MARA University of Technology, Shah Alam 40450, Malaysia (E-mail: nurulaqilahabdul@gmail.com)

**Professor, Bioremediation Research Centre (myBioREC), The MARA University of Technology, Shah Alam 40450, Malaysia (E-mail: suhaimi.talib@intec.edu.my)

***Senior Lecturer, Bioremediation Research Centre (myBioREC), The MARA University of Technology, Shah Alam 40450, Malaysia (Corresponding Author, E-mail: amnorzahira@salam.uitm.edu.my)

et al., 2010). Literature has reported that pH condition in groundwater was in the range of pH 5 to 9 due the complex biogeochemistry conditions of groundwater (e.g., microbial population, electrolytes and soil minerals) (Schwartz and Kgomanyane, 2008). Removal of Cr^{6+} by iron reductant (e.g., nano zero valent iron (nZVI) and magnetite) was significantly decreased as the pH increased from pH 5 to 9 due to the oxidation of Fe^{2+} to ferric iron (Fe^{3+}) (Amir and Lee, 2011; Giraldo, Erto, and Moreno-Piraján, 2013; He and Traina, 2005). However, nano-FeS_2 contained disulfide (S_2^{2-}) and it may have higher reactivity at alkaline condition. Humic Acid (HA) is one of the main compound of NOM in the groundwater and it can exist in soluble or colloidal forms depending on solution conditions. HA significantly adsorbed on the surface of iron reductant (e.g., Fe^{2+} and Fe^{3+}) because it has anionic functional groups (e.g., carboxylic and phenol groups) that may lead to the formation of new complexation species on the surface of iron reductant (Lalonde *et al*., 2012; Tombácz *et al*., 2004). This finding indicates that redox reaction between Fe^{2+} and Cr was inhibited and influenced the removal kinetic rate of Cr. Literatures have reported that the reduction of Cr by iron-reductant was decreased in the present of HA (Dries *et al*., 2005; Mak *et al*., 2009). However, there is an argument on the reaction mechanisms of the reduction of Cr by nano-FeS_2 and other iron-reductants due to the different chemical composition (e.g., Fe^{2+} and S^{2-}). The argument on the reduction of Cr^{6+} to Cr^{3+} by nano-FeS_2 is probably controlled predominantly by S^{2-} compared to Fe^{2+} under different environmental conditions are currently in debate. Fundamental study on the role of S^{2-} in nano-FeS_2 is urgently required. The fate of reduction of Cr^{6+} to Cr^{3+} by nano-FeS_2 under different environmental conditions (e.g., suspension pH and humic acid) is not well reported. The main objective of this study is to investigate removal of Cr^{6+} by nano-FeS_2 under different environmental conditions. Surface characterization of nano-FeS_2 was measured to understand potential reaction mechanisms during removal of Cr^{6+} by nano-FeS_2. This research provides better understanding on the fate of Cr^{6+} in the presence of nano-FeS_2 under different environmental conditions.

2. Materials and Method

2.1 Chemicals

Chemicals used include chromium (SpectrosoL, 1000 mg/L), nano-FeS_2 (FeS_2, Sigma Aldrich, Germany, 99%), humic acid (HA) (Technical, Sigma Aldrich, Germany), 2-(N-Morpholino) ethanesulfonic acid hydrate 4 hydroxide Morpholineethanesulfonic acid (MES hydrate, Sigma Aldrich, Germany, 99.5%) and Trizma (Tris, Sigma Aldrich, Germany 9.99%). Hydrochloric acid (HCl, ChemAR, 98%) and sodium (NaOH), analytical reagent grade, Fisher Scientific, USA) used as pH modifiers. Ultra-pure water (UPW, 18.2MΩ, Alga Purelab Ultra, United Kingdom) purged with nitrogen gas (N_2) before used for 30 minutes to eliminate dissolved oxygen. Anaerobic chamber (Plus Labs, Coy Laboratory Product Inc, USA) maintained purged with 95% N_2. Glassware were washed using ChemPur Alkaline, Liquid Laboratory Cleanser, rinsed with tap water, soaked in 15% Nitric acid for 24 hours and rinsed with UPW.

2.2 Experimental Procedure

Batch experiments were used to investigate the effectiveness of Cr_T removal by nano-FeS_2. Preparation of controls and samples were performed in the anaerobic chamber. Biological buffer solutions (50 mM MES and 50 mM Trizma buffer) were used to maintain the suspension at pH 5, 7 and 9. Biological buffer was poured into 40 mL amber vials containing nano-FeS_2. 1 mg/L of Cr_T concentration was prepared from 1,000 mg/L Cr_T stock solution and spiked into the vial containing biological buffer and nano-FeS_2. Vials were rotated at 7 rpm for 2 to 30 minutes in the anaerobic chamber and were quickly transferred to centrifuge. Samples were centrifuge at 5,000 rpm for 15 minutes and the supernatant was analyzed.

In order to identify the fate of reduction of Cr_T by nano-FeS_2 under different environmental conditions, removal of Cr_T by nano-FeS_2 under different concentrations of Cr_T and nano-FeS_2, different suspension pH and in the presence of humic acid were conducted. To investigate the effect of concentration of Cr_T, batch experiments were carried out under the different Cr_T concentration (1.0 mg/L, 1.5 mg/L and 2 mg/L) with the fixed concentration of the nano-FeS_2 (1.25 g/L) at pH 7. To reveal the effects of the nano-FeS_2 concentration on the removal of Cr_T by nano-FeS_2, different concentration of nano-FeS_2 (0.75 g/L, 1.0 g/L and 1.25 g/L) were added into the vials and Trizma buffer solution was poured to keep the suspension pH constant at pH 7. 1 mg/L of Cr_T was spiked into the vials to initiate reaction. To examine the effect of pH on the removal of Cr_T by nano-FeS_2, different pH buffers (pH 5, pH 7 and pH 9) were prepared using MES and TRIS and adjusted using NaOH and HCl. pH meter (827 pH Lab Metrohm, Switzerland) was used to check the pH buffer and poured into vials that contained 1.25 g/L of nano-FeS_2. To investigate the effect of HA on the removal of Cr_T by nano-FeS_2, two different concentrations of HA (0.25 g/L and 1.25 g/L) were prepared and added into the vials containing 3.75 g/L of nano-FeS_2. 50 mM of TRIS buffer solution was prepared and poured into the vials and 1 mg/L of Cr_T was spiked into the vials to initiate reaction. Duplicate batch experiments were run in two (2) sets of independent to confirm reproducibility of the experimental results. The removal kinetic of Cr_T by nano-FeS_2 can be calculated using Eq. (1) below:

$$C = C_o e^{-kt} \tag{1}$$

where C is the concentration of Cr_T at time (mg/L), C_0 is the initial concentration of Cr_T, k is the pseudo-first-order constant (min^{-1}), and t is the reaction time.

2.3 Analytical Procedure

Cr_T concentrations were analyzed with flame atomic absorption spectroscopy (FAAS, Perkin Elmer®, AAnalyst™ 800-Waltham, MA, USA) calibrated with Cr standard solutions (Perkin Elmer, 1,000 mg/L) with concentrations ranging from 0.2 to 2 mg/L. A chromium hollow cathode lamp (25 mA) was employed and flame was used for atomizing the sample. Air (17.0 L/min) and acetylene (2.7 L/min) were used in conjunction with a measurement line of 359.35 nm. Field emission scanning electron microscope (FESEM, Supra 40 VP, Carl Zeiss, Germany) in conjunction with energy-dispersive X-Ray spectroscopy (EDS, INCA PentaFETx3 detector, Oxford Instruments, UK) was used to analyze surface morphology and element composition of the surface of nano-FeS_2 before the kinetic reaction to determine its purity and chemical functional group involved in the reaction. The surface charge of nano-FeS_2 was analyzed with Malvern Zetasizer Nano Series Instrument (United Kingdom). The samples was also characterized by X-Ray Diffraction (XRD) using the PANalytical X'pert Pro MPD diffractometer for phase and purity studies. Attenuated total reflection (ATR-FTIR, Perkin-Elmer®, Spectrum 400-Waltham, MA, USA) spectrometer was used to identify functional groups.

3. Result and Discussion

3.1 Characterization Study of Nano-FeS_2 Particles

3.1.1 SEM Analysis

Figure 1(a) shows the image of nano-FeS_2 particles using SEM-EDX. The SEM-EDX images show that most of nano-FeS_2 particles sizes were in the range of 50 nm to 100 nm, indicating that FeS_2 particles are nano-size and may provide higher reactive surface compared to micro-size of FeS_2. Fig. 1(b) shows the SEM-EDX image spectra of chemical composition of nano- FeS_2 particles. This result reveals that nano-FeS_2 particles contain iron (Fe) and sulphur (S).

Table 1 shows the composition of Fe and S was 53.10% and 46.90% respectively. This result indicates that Fe is predominant compared to S. This result suggests that nano-FeS_2 particles in this study may provide high reactive surface that contain ferrous ion (Fe^{2+}) and sulphide (S^{2-}), which can enhance removal kinetic of Cr_T by nano-FeS_2 particles.

Table 1. Chemical Composition of Nano-FeS_2 Particles

Elements	Concentration	
	Weight percentage	Atomic percentage
Sulfur	46.90	60.60
Iron	53.10	39.40
Total	100	

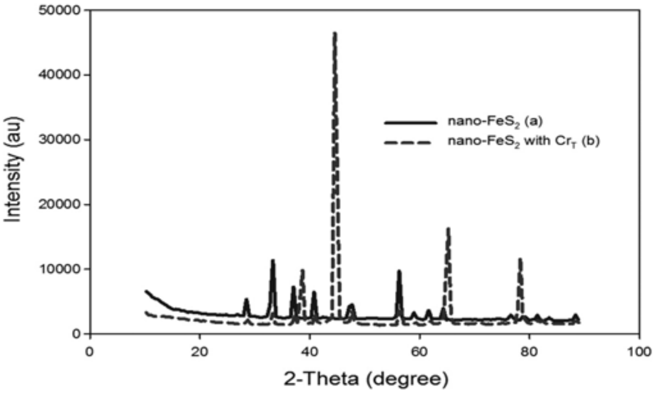

Fig. 2. XRD Patterns of the Nano-FeS_2: (a) before, (b) after Cr_T Adsorbed

3.1.2 XRD Analysis

Figure 2 illustrates XRD diffractogram of nano-FeS_2 used in this experiment before and after adsorption with Cr_T. XRD analysis shows that typical diffraction peaks of 2θ at 28.46°, 33.28°, 37.0°, 40.77°, 59.0° and 64° indicates the crystalline nano-FeS_2 are clearly observed and highly pure. This result confirms that Fe and S in nano-FeS_2 mainly existed as FeS_2 and it is consistent with the SEM-EDX results. The XRD patterns obtained from the analysis indicate that all the peaks were matched with the library database patterns of faced cubic center (FCC) nano-FeS_2 as shown in the Fig. 2(a). This experimental results is similar with XRD analysis reported in a previous study (Kim *et al*., 2002). However, the XRD pattern of nano-FeS_2 adsorbed with Cr_T (Fig. 2(b)) shows a slightly different pattern compared to nano-FeS_2 alone. There were three obvious different diffraction peaks at 44.5°, 65.3° and 78.33°, suggesting that new

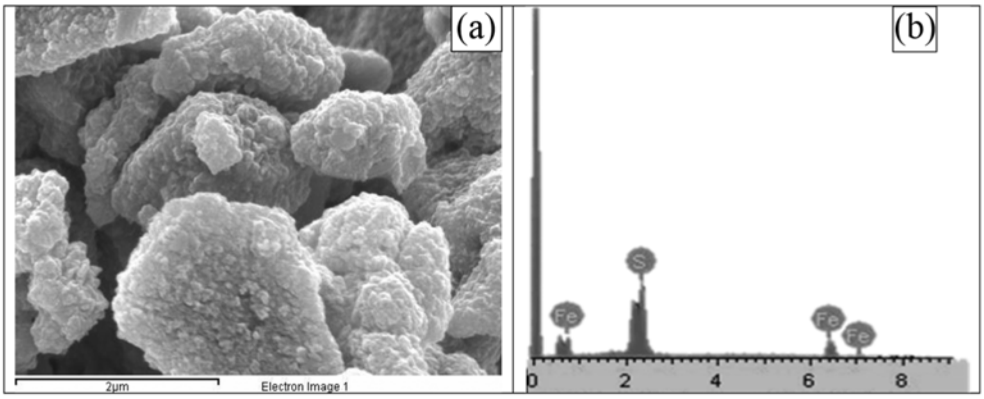

Fig. 1. Loading Apparatus and Photo: (a) SEM Image of Nano-FeS_2, (b) EDX Image of Nano-FeS_2

chemical speciation may form on the surface of nano-FeS_2 after reaction with Cr_T which is referred to iron chromite oxide ($FeCr_2O_4$) and it match well with the library database. It has been reported that $FeCr_2O_4$ was also formed on the surface of magnetite during the removal reaction of Cr with magnetite (Hu *et al*., 2004). Formation of Cr^{3+} as products of Cr^{6+} reduction by FeS_2 may precipitate as $Cr(OH)_{3(s)}$ and/or mixed of $Fe\text{-}Cr(OH)_{3(s)}$ under different conditions (e.g, pH and concentration of Cr) (Kantar *et al*., 2015). The oxidation products (e.g., $Fe(OH)_{3(s)}$, $Cr(OH)_{3(s)}$, $Fe\text{-}Cr(OH)_{3(s)}$) can be accumulated on the surface of FeS_2 and formed a passivating layer (Kantar *et al*., 2015). This experimental finding clearly proved that secondary mineral was formed on the surface of nano-FeS_2, indicating that adsorption, complexation and reduction reactions may occur during the removal reaction.

3.2 Removal of Cr_T by Nano-FeS_2 under Different Initial Concentration of Cr_T

Figure 3 shows the Cr_T removal by nano-FeS_2 under three (3) different Cr_T concentrations (1 mg/L, 1.5 mg/L and 2 mg/L). Removal kinetic rate constant of Cr_T by nano-FeS_2 was fitted by a pseudo-first-order kinetic model ($R^2 = 0.96$). Experimental result shows that the Cr_T removal decreased as the initial concentration of Cr_T increased from 1 mg/L to 2 mg/L. Completed removal of 1 mg/L of Cr_T by nano-FeS_2 was observed in 20 minutes. Approximately 64.33% and 68.50% of Cr_T were removed at 1.5 mg/L and 2.0 mg/L of Cr_T respectively within 10 minutes of reaction time and then plateau phase is reached which lasted to the end of the experiment. This result indicates that no significant removal of Cr_T by nano-FeS_2 was observed after 10 minutes reaction time. This is due to the limited reactive surface available on the surface of nano-FeS_2. Slope of the linear regression line shows a proportional decreased between the rate constant and the initial Cr_T concentration (1 mg/L to 2 mg/L) (Fig. 3(inset)). An estimated removal kinetic rate constant for the removal of Cr_T by nano-FeS_2 (1.25 g/L) was $k = 0.43$ min^{-1} at 1 mg/L of the Cr_T concentration. Removal kinetic rate constant decreased to $k = 0.39$ min^{-1} and $k = 0.30$ min^{-1} when Cr_T concentration increased to 1.5 mg/L and 2 mg/L respectively. The result suggests that nano-FeS_2 particles has limited reactive surface as the concentration of the Cr_T increased. The findings of this study are consistent with the experimental result reported by from a previous study by Kantar *et al.* (2015). Removal kinetic rate constant of Cr^{6+} was decreased as the concentration of Cr^{6+} was increased, indicating that there are limited number of reactive surface sites on nano-FeS_2 (Kantar *et al*., 2015). According to Graham and Bouwer (2012), reduction of Cr^{6+} on the surface of nano-FeS_2 significantly correlated with reactive site of nano-FeS_2 ($[Cr^{6+}]$)/ [FeS_2 reactive sites]. Excess surface sites of nano-FeS_2 leads to complete removal of Cr^{6+} via first order reaction kinetics (Graham and Bouwer, 2012).

3.3 Removal of Cr_T by Nano-FeS_2 under Different Concentration of Nano-FeS_2 Particles

Figure 4 demonstrates the effect of the nano-FeS_2 concentration on the removal of Cr_T by nano-FeS_2 at suspension pH 7. Removal of 1.0 mg/L of Cr_T by nano-FeS_2 was increased as the concentration of nano-FeS_2 increased from 0.75 g/L to 1.0 g/L and 1.25 g/L in 30 minutes reaction time. A complete removal of 1.0 mg/L of Cr_T by nano-FeS_2 was observed at 1.25 mg/L of nano-FeS_2 in 20 minutes reaction time. Approximately 92.7% and 66% of Cr_T were removed by 1.0 g/L and 0.75 g/L of nano-FeS_2 respectively in 30 minutes. Experimental result shows that rapid removals of Cr_T at different concentrations of nano-FeS_2 were observed in the first 10 minutes and then the removal of Cr_T started to slow and shows the plateau phase. Similar experimental result was reported in a previous study (Zouboulis *et al*., 1995). The kinetic data of Cr_T removals by nano-FeS_2 particle were fitted by a pseudo-first-order kinetic model ($R^2 = 0.82$). Fig. 4(inset)

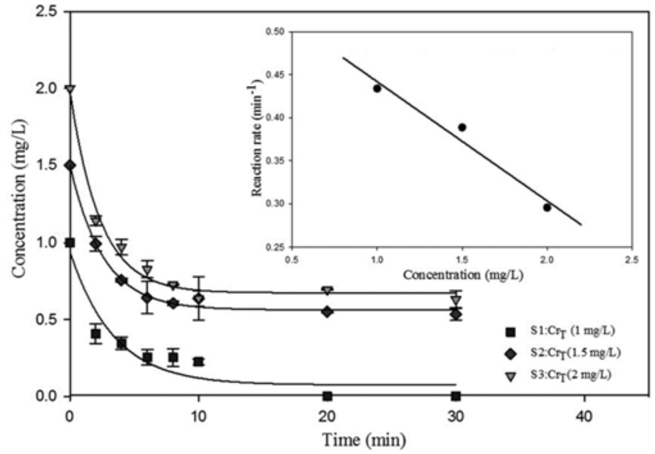

Fig. 3. Effect of Initial Concentration of Cr_T on Removal Kinetic of Cr_T by Nano-FeS_2 Particles. Concentration of Nano-FeS_2 = 1.25 g/L, Suspension pH =7. Fig. 3(Inset): Removal Kinetics Rate Constant (k) of CrT by Nano-FeS_2 under Different Concentrations of Cr_T

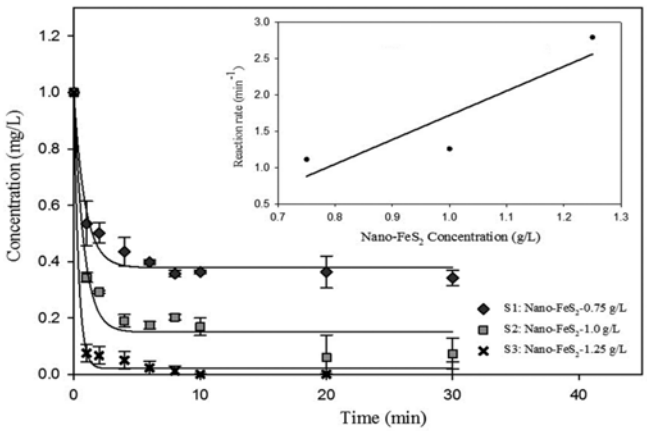

Fig. 4. Effect of Nano-FeS_2 Concentration on Removal Kinetic of Cr_T by Nano-FeS_2 Particles. Initial Concentration of Cr_T = 1 mg/L, pH Solution = pH 7. Fig. 4 (inset): Removal Kinetic Rate Constant (k) of Cr_T at Different Nano-FeS_2 Concentrations

shows removal kinetic rate constant of Cr_T under different concentration of nano-FeS_2 (0.75 g/L to 1.25 g/L). Slope of the linear regression line shows a proportional increased between the rate constant and the added nano-FeS_2 concentration. This result indicates that removal kinetic of Cr_T by nano-FeS_2 was significantly increased as the concentration of nano-FeS_2 increased probably due to the greater reactive surface area provided by nano-FeS_2 at higher concentration of nano-FeS_2 (Amir and Lee, 2011). An estimated removal kinetic rate constant for the removal of Cr_T by nano-FeS_2 at 0.75 g/L was $k = 1.11$ min^{-1} and it increased as the concentration of nano-FeS_2 was increased from 0.75 g/L to 1.0 g/L and 1.25 g/L. The removal kinetic rate constant of Cr_T at 1.0 g/L of nano-FeS_2 was $k = 1.26$ $mins^{-1}$, which is 1.13 times greater than that at 0.75 g/L of nano-FeS_2. Additional of 1.25 g/L of nano-FeS_2 significantly increased the removal kinetic rate constant of Cr_T by nano-FeS_2 2.21 times greater ($k = 2.8$ $mins^{-1}$) at 1.0 g/L of nano-FeS_2. This experimental result suggests that high concentration of nano-FeS_2 significantly provides sufficient surface reactive area to allow adsorption and reduction of Cr_T to Cr^{3+}. Due to this reason, removal kinetic of Cr_T was significantly increased as the concentration of nano-FeS_2 increased from 0.75 g/L to 1/25 g/L. This experimental result was consistent with the experimental results reported by Lin and Huang (2008).

3.4 Effect of pH on Cr_T Removal by Nano-FeS_2

Figure 5 demonstrates the removal of Cr_T by nano-FeS_2 under different suspension pH (pH 5, 7, 9). The removal kinetics data of Cr_T by nano-FeS_2 under different suspension pH were fitted by a pseudo-first-order kinetic model ($R^2 = 0.63$). It is noteworthy that the removal of the Cr_T by nano-FeS_2 was significantly increased as the suspension pH increased (pH 5-9). An approximately 93% of Cr_T was removed by nano-FeS_2 at suspension pH 9, followed by 80.36% and 40.35% removal of Cr_T by nano-FeS_2 at suspension pH 5 and suspension pH 6, respectively. This experimental finding indicates that the removal of Cr_T by nano-FeS_2 was greater under alkaline condition than neutral condition. This experimental results suggests that reactive surface of nano-FeS_2 is dominated by sulfide (S^{2-}) compared to ferrous (Fe^{2+}). Literatures have reported that S^{2-} has higher nucleophilicity under alkaline condition and may enhance reduction of Cr_T (Amir and Lee, 2012). Fig. 5(inset) shows that removal kinetic rate constant of Cr_T by nano-FeS_2 under different suspension pH. Removal kinetic rate constant accelerated as the initial suspension pH increased between pH 5 to pH 9. The removal kinetic rate constant of Cr_T by nano-FeS_2 at pH 9 (3.02 min^{-1}) was 6 times greater than that at pH 7 (0.51 min^{-1}), suggesting that reactive surface area of nano-FeS_2 was significantly increased under alkaline condition. The lowest removal kinetic rate constant of Cr_T by nano-FeS_2 was observed at suspension pH 5 (0.86 min^{-1}), indicating that surface reactivity of nano-FeS_2 was less reactive compared to the neutral and alkaline conditions. This experimental result was consistent with the experimental results reported by Amir and Lee (2011). Surface charge of nano-FeS_2 was further characterized using Zeta Potential analysis.

Figure 6 demonstrates surface charge of nano-FeS_2 with and without Cr_T under different suspension pH (pH 3-9). Surface charge of nano-FeS_2 in the absence of Cr_T was positive (+10.3 mV to +11.2 mV) at acidic condition (pH 3-5). This result suggests that the surface of nano-FeS_2 was protonated with H^+ under acidic condition and potential chemical species that may presence are ferric hydroxide ($\equiv FeOH_3^+$) and ferric sulfide ($\equiv FeSH_3^+$) (Lin and Huang, 2008). However, surface charge of nano-FeS_2 was drastically decreased between pH 5 and pH 6.10 (P_{ZPC}), due to Zero Point Charge (ZPC) condition of nano-FeS_2. It has been reported that P_{ZPC} of nano-FeS_2 was in the range of pH 6.2 to 7.0 (Bae *et al*., 2012). Surface charge of nano-FeS_2 was significantly negative between pH 7 and pH 9 (-6.22 mV, -11.4 mV and -13.8mV). This result suggests that surface of nano-FeS_2 was deprotonated and there is potential presence of ferrous oxide ($\equiv FeO^-$) and ferrous sulfide ($\equiv FeS^-$) (Amir and Lee, 2012; Bae *et al*., 2012). Due to this reason, reduction of Cr_T to Cr^{3+} is greater

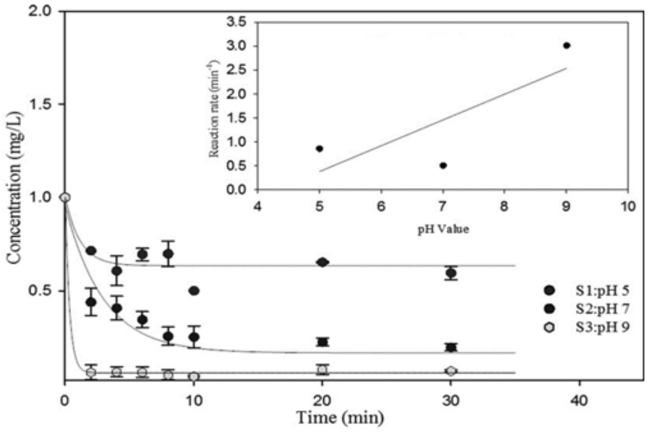

Fig. 5. Effect of pH on Cr_T Removal by Nano-FeS_2 Particles. Initial Concentration of Cr_T = 1 mg/L, pH Solution = 5, 7 and 9. Fig. 5(inset): Removal Kinetic Rate Constant (k) of CrT by nano-FeS_2 under Different Suspension pH

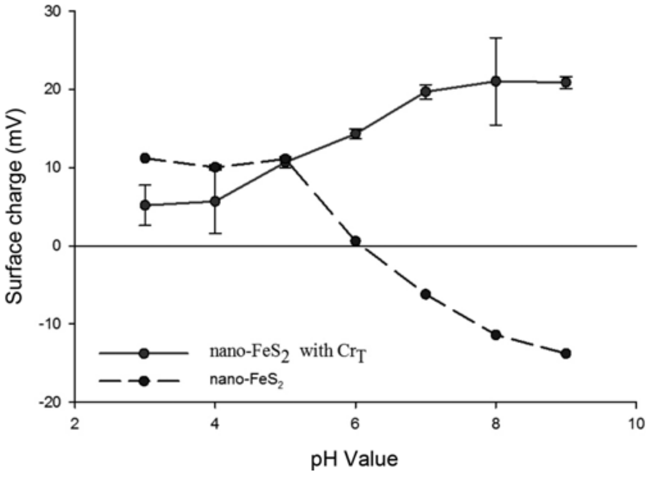

Fig. 6. Surface Charge (mV) of Nano-FeS_2 as a Function of pH in the Absence and Presence of the Cr_T between pH Range of 3–9. Initial Concentration of Nano-FeS_2 = 1.25 g/L

under neutral and alkaline conditions than that at under acidic condition. Surface charge characteristic of nano-FeS_2 with Cr_T was contradictory with the surface charge of nano-FeS_2 without Cr_T. Surface charge of nano-FeS_2 remained positive under all suspension pH conditions where the surface charge of nano-FeS_2 was in the range of 5.1 mV to 20.9 mV. This result suggests that adsorption of Cr_T on the surface of nano-FeS_2 significantly altered the originality surface charge of nano-FeS_2. This experimental finding reveals that the reactive surface area of nano-FeS_2 significantly depends on its surface charge and type of chemical species under different suspension pH.

3.5 Effect of Humic Acid on the Removal of Cr_T by Nano-FeS_2 Particles

Figure 7 shows the effect of HA on the removal of Cr_T by nano-FeS_2 at pH 7. Experimental result shows that the removal of Cr_T by nano-FeS_2 alone was greater than that in the presence of HA. Removal of Cr_T by nano-FeS_2 was significantly greater than that by nano-FeS_2 in the present of HA over in 30 minutes at pH 7. An approximately 92.40% (k = 0.24 min^{-1}) of Cr_T was removed by nano-FeS_2 in the absence of HA in 30 minutes reaction time. An approximately 20% of Cr_T was removed by nano-FeS_2 in the present of 0.25 g/L and 1.25 g/L of HA in 30 minutes. No significant different between the removal kinetic rate constant of Cr_T by nano-FeS_2 at 0.25 g/L (k = 0.72 min^{-1}) and 1.25 g/L (k = 0.50 min^{-1}) of HA. This result indicates that the reduction of Cr_T by nano-FeS_2 was inhibited due to the adsorption of HA on the surface of nano-FeS_2. This result was consistent with the experimental finding from the previous study (Rao *et al*., 2009; Tsang, 2014). Previous studies have reported that removal of arsenic by Fe^o was inhibited due to the formation of new complexation species between Fe^0 and humic acid (Rao *et al*., 2009; Tsang, 2014).

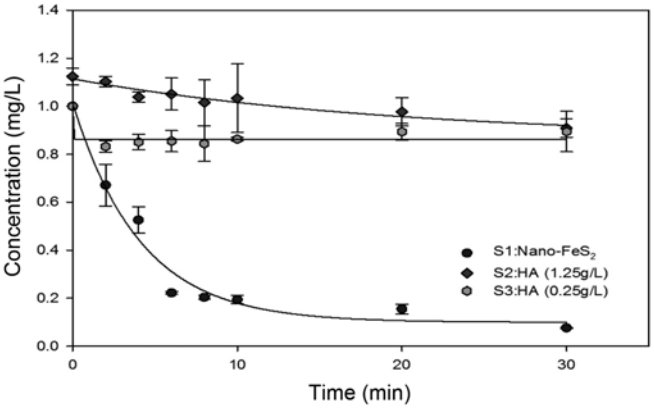

Fig. 7. Effect of HA on Removal of Cr_T by Nano-FeS_2 Particles. Initial Concentration = 1 mg/L, pH Solution = pH 7

Table 2. FTIR Absorption Bands of the Humic Acid

Assignment	Wavenumber (cm^{-1})
	Humic acid
Carbonyl group (COO^-)	1575.15 cm^{-1}
	1374.59 cm^{-1}

Table 2 shows FTIR analysis on the anionic functional group present in HA. Carbonyl group (COO^-) was detected at wavelength 1575.15 cm^{-1} and 1374.59 cm^{-1}, suggesting that new complex species between Fe^{2+} and COO^- may occur and inhibit the removal of Cr_T by nano-FeS_2. This experimental result was very significant to identify potential reaction mechanism that may occur during the removal of Cr_T by nano-FeS_2 in the presence of humic acid.

4. Conclusions

Finding from this study proved that nano-FeS_2 particles are capable of removing Cr_T under different concentration of nano-FeS_2, Cr_T, humic acid and suspension pH. Surface of nano-FeS_2 particles in this study was reactive because Fe (53.10%) and S (46.90%) were the main chemical compounds on the surface of nano-FeS_2. Removal kinetic rate constant of Cr_T by nano-FeS_2 was significantly controlled by the reactive surface area of nano-FeS_2 under any environment condition. Removal kinetic of Cr_T by nano-FeS_2 was significantly increased at 1.25 g/L of nano-FeS_2 (2.78 $mins^{-1}$) and alkaline condition (3.01 $mins^{-1}$). However, the removal kinetics rate constant of Cr_T was significant decreased in the present of humic acid (k = 0.72 min^{-1}) and at high concentration of Cr_T (0.29 $mins^{-1}$). Based on the experimental findings, the optimum conditions for significant removal of Cr_T by nano-FeS_2 are at pH 9 and concentrations of Cr_T, nano-FeS_2 and humid acid are 1 mg/L, 1.25 g/L and less than 0.25 g/L (> [0.25]). However, removal of Cr_T by nano-FeS^2 through adsorption reaction may inhibit and enhance due to the existence of other biogeochemistry factors in groundwater (e.g., enzyme from bacteria and electrolytes) (Mak *et al*., 2009). Reactive surface area of nano-FeS_2 significantly depends on its surface charge and type of complexation species under different environmental conditions. Surface charge of nano-FeS_2 alone was significantly altered under different suspension pH and in the presence of Cr_T and HA. Identification of formation of new complexation species on the surface of nano-FeS_2 in the present of Cr_T reveals that adsorption, complextion and reduction reactions may occur during the removal reaction. This study provides fundamental knowledge on the fate of Cr in the present of nano-FeS_2 alone, nano-FeS_2 with HA and under different suspension pH. Finding from this study can be used to enhance remediation technology to removal heavy metals in soil and groundwater. Reaction mechanisms on removal of Cr_T by nano-FeS_2 can by be applied at the remediation sites to advanced natural attenuation and nano-FeS_2-based ex-situ soil and groundwater treatments (e.g., permeable reactive barrier).

Acknowledgements

This study was funded by Universiti Teknologi MARA (600-IRMI/MYRA 5/3/GIP (011/2017)) through the Project Kinetic and Adsorption Modeling Studies on the Removal of Chromium Using nano-FeS$_2$. Author greatly acknowledge Faculty of Civil Engineering for analytical support, laboratory assistant and myBioREC members.

References

Aftabtalab A, Sadabadi H (2014). "Application of Magnetite (Fe$_3$O$_4$) Nanoparticles in Hexavalent Chromium Adsorption from Aquatic Solutions." *J Pet Environ Biotechnol,* Vol. 6, No. 2, pp. 1-3, DOI: 10.4172/2157-7463.1000200.

Amir, A. and Lee, W. (2011). "Enhanced reductive dechlorination of tetrachloroethene by nano-sized zero valent iron with vitamin B 12." *Chemical Engineering Journal*, Vol. 170, Nos. 2-3, pp. 492-497, DOI: 10.1016/j.cej.2011.01.048.

Amir, A. and Lee, W. (2012). "Enhanced reductive dechlorination of tetrachloroethene during reduction of cobalamin (III) by nano-mackinawite." *Journal of Hazardous Materials*, Vols. 235-236, pp. 359-366, DOI: 10.1016/j.jhazmat.2012.08.017.

Bae, S., Mannan, M. B., and Lee, W. (2012). "Adsorption of cationic cetylpyridinium chloride on pyrite surface." *Journal of Industrial and Engineering Chemistry*, Vol. 18, No. 4, pp. 1482-1488, DOI: 10.1016/j.jiec.2012. 02.010.

Banks, M. K., Schwab, A. P., and Henderson, C. (2006). "Leaching and reduction of chromium in soil as affected by soil organic content and plants." *Chemosphere*, Vol. 62 No. 2, pp. 255-264, DOI: 10.1016/ j.chemosphere.2005.05.020.

Cook, K. R. (2000). *In situ treatment of soil and groundwater contaminated with chromium - Technical resource guide,* EPA/625/r-00/005 (NTIS PB2001-103721).

Demoisson, F., Mullet, M., and Humbert, B. (2007). "Investigation of pyrite oxidation by hexavalent chromium: Solution species and surface chemistry." *Journal of Colloid and Interface Science*, Vol. 316, No. 2, pp. 531-540, DOI: 10.1016/j.jcis.2007.08.011.

Demoisson, F., Mullet, M., and Humbert, B., Demoisson, F., Mullet, M., and Humbert, B. (2005). "Pyrite oxidation by hexavalent chromium: Investigation of the chemical processes by monitoring of aqueous metal species." *Environmental Science and Technology*, Vo. 39, No. 22, pp. 8747-8752, DOI: 10.1021/es050717s.

Dries, J., Bastiaens, L., Springael, D., Kuypers, S., Agathos, S. N., and Diels, L. (2005). "Effect of humic acids on heavy metal removal by zero-valent iron in batch and continuous flow column systems." *Water Research*, Vol. 39, No. 15, pp. 3531-3540, DOI: 10.1016/ j.watres.2005.06.020.

Ertani, A., Mietto, A., Borin, M., and Nardi, S. (2017). "Chromium in agricultural soils and crops: A review." *Water, Air, and Soil Pollution*, Vol. 228, No. 5, DOI: 10.1007/s11270-017-3356-y.

Giraldo, L., Erto, A., and Moreno-Piraján, J. C. (2013). "Magnetite nanoparticles for removal of heavy metals from aqueous solutions: Synthesis and characterization." *Adsorption* Vol. 19, pp. 465-474, DOI: 10.1007/s10450-012-9468-1.

Graham, A. M. and Bouwer, E. J. (2012). "Oxidative dissolution of pyrite surfaces by hexavalent chromium: Surface site saturation and surface renewal." *Geochimica et Cosmochimica Acta*, Vol. 83, pp. 379-396, DOI: 10.1016/j.gca.2012.01.006.

He, Y. T. and Traina, S. J. (2005). "Cr(VI) reduction and immobilization by magnetite under alkaline pH conditions: The role of passivation." *Environmental Science and Technology*, Vol. 39, No. 12, pp. 4499-4504, DOI: 10.1021/es0483692.

Hu, J., Lo, I. M. C., and Chen, G. (2004). "Removal of Cr(VI) by magnetite nanoparticle." *Water Science and Technology*, Vol. 50, No. 12, pp. 139-146.

Kantar, C., Ari, C., Keskin, S., Dogaroglu, Z. G., Karadeniz, A., and Alten, A. (2015). "Cr(VI) removal from aqueous systems using pyrite as the reducing agent: Batch, spectroscopic and column experiments." *Journal of Contaminant Hydrology*, Vol. 174, pp. 28-38, DOI: 10.1016/j.jconhyd.2015.01.001.

Kim, J. G., Jung, P.-K. K., Moon, H.-S. S., and Chon, C.-M. M. (2002). "Reduction of hexavalent chromium by pyrite-rich andesite in different anionic solutions." *Environmental Geology*, Vol. 42, No. 6, pp. 642-648, DOI: 10.1007/s00254-002-0567-2.

Lalonde, K., Mucci, A., Ouellet, A., and Gélinas, Y. (2012). "Preservation of organic matter in sediments promoted by iron." *Nature*, Vol. 483, pp. 198-200, DOI: 10.1038/nature10855.

Lasheen, M. R., El-Sherif, I. Y., Sabry, D. Y., El-Wakeel, S. T., and El-Shahat, M. F. (2013). "Removal and recovery of Cr (VI) by magnetite nanoparticles." *Desalination and Water Treatment*, Vol. 52, Nos. 34-36, pp. 6464-6473.

Lin, Y. T. and Huang, C. P. (2008). "Reduction of chromium (VI) by pyrite in dilute aqueous solutions." *Separation and Purification Technology*, Vol. 63, No. 1, pp. 191-199, DOI: 10.1016/j.seppur. 2008.05.001.

Liu, Y., Mou, H., Chen, L., Mirza, Z. A., and Liu, L. (2015). "Cr(VI)-contaminated groundwater remediation with simulated Permeable Reactive Barrier (PRB) filled with natural pyrite as reactive material: Environmental factors and effectiveness." *Journal of Hazardous Materials*, Vol. 298, No. 4, pp. 83-90, DOI: 10.1016/j.jhazmat.2015. 05.007

Mak, M. S. H., Rao, P., and Lo, I. M. C. (2009). "Effects of hardness and alkalinity on the removal of arsenic (V) from humic acid-deficient and humic acid-rich groundwater by zero-valent iron." *Water Research*, Vol. 43, No. 17, pp. 4296-4304, DOI: 10.1016/j.watres.2009.06.022.

Mohan, D. and Pittman, C. U. (2006). "Activated carbons and low cost adsorbents for remediation of tri- and hexavalent chromium from water." *Journal of Hazardous Materials*, Vol. 137, Issue 2, pp. 762-811, DOI: 10.1016/j.jhazmat. 2006. 06.060.

Panagiotakis, I., Dermatas, D., Vatseris, C., Chrysochoou, M., Papassiopi, N., Xenidis, A., and Vaxevanidou, K. (2015). "Forensic investigation of a chromium (VI) groundwater plume in Thiva, Greece." *Journal of Hazardous Materials*, Vol. 281, pp. 27-34, DOI: 10.1016/j.jhazmat. 2014.09.048.

Porsch, K., Dippon, U., Rijal, M. L., Appel, E., and Kappler, A. (2010). "In-situ magnetic susceptibility measurements as a tool to follow geomicrobiological transformation of Fe minerals." *Environmental Science and Technology*, Vol. 44, No. 10, pp. 3846-3852, DOI: 10.1021/es903954u.

Rao, P., Mak, M. S. H., Liu, T., Lai, K. C. K., and Lo, I. M. C. (2009). "Chemosphere Effects of humic acid on arsenic (V) removal by zero-valent iron from groundwater with special references to corrosion products analyses." *Chemosphere*, Vol. 75, No. 2, pp. 156-162, DOI: 10.1016/j.chemosphere.2008.12.019.

Schwartz, M. O. and Kgomanyane, J. (2008). "Modelling natural attenuation of heavy-metal groundwater contamination in the Selebi-Phikwe mining area, Botswana." *Environmental Geology*, Vol. 54, No. 4, pp. 819-830, DOI: 10.1007/s00254-007-0865-9.

Sharma, S. K. (2001). *Adsorptive iron removal from groundwater, CRC Press.*

Taylor, P. A. (2015). "Physical, chemical, and biological treatment of groundwater at contaminated nuclear and NORM sites." *Environmental*

Remediation and Restoration of Contaminated Nuclear and Norm Sites. Elsevier Ltd., pp. 237-256, DOI: 10.1016/B978-1-78242-231-0.00010-7.

Tombácz, E., Libor, Z., Illés, E., Majzik, A., and Klumpp, E. (2004). "The role of reactive surface sites and complexation by humic acids in the interaction of clay mineral and iron oxide particles." *Organic Geochemistry*, Vol. 35, No. 3, pp. 257-267, DOI: 10.1016/j.orggeochem.2003.11.002.

Tsang, D. C. W. (2014). "Influence of natural organic matter on contaminant removal by permeable reactive barrier." *The Role of Colloidal Systems in Environmental Protection*. Elsevier B.V., pp. 19-40, DOI: 10.1016/B978-0-444-63283-8.00002-8.

Vinuth, M., Bhojya Naik, H. S., and Manjanna, J. (2015). "Remediation of hexavalent chromium from aqueous solution using clay mineral Fe(II)-montmorillonite: Encompassing anion exclusion impact." *Applied Surface Science*, Vol. 357, pp. 1244-1250, DOI: 10.1016/j.apsusc.2015.09.167.

Wernberg, T. (2017). "Multicomponent groundwater transport with chemical equilibrium and kinetics: Model development and evaluation." *Hydrological Sciences Journal*, Vol. 43, No. 2, pp. 299-317, DOI: 10.1080/02626669809492123.

Zouboulis, A. I., Kydros, K. A., and Matis, K. A. (1995). "Removal of hexavalent chromium anions from solutions by pyrite fines." *Water Research*, Vol. 29, No. 7, pp. 1755-1760, DOI: 10.1016/0043-1354(94)00319-3.